

BÉZIER CURVES THAT ARE CLOSE TO ELASTICA

DAVID BRANDER, JAKOB ANDREAS BÆRENTZEN, ANN-SOFIE FISKER, AND JENS GRAVESEN

ABSTRACT. We study the problem of identifying those cubic Bézier curves that are close in the L^2 norm to planar elastic curves. We identify an easily computable quantity, which we call the λ -residual e_λ , that accurately predicts a small L^2 distance. Using this, we identify geometric criteria on the control polygon that guarantee that a Bézier curve is within 1% of its arc-length to an elastic curve. Finally we give two projection algorithms that take an input Bézier curve and adjust its length, whilst keeping the end-points and end-tangent angles fixed, until it is close to an elastic curve.

1. INTRODUCTION

Bézier curves, and their generalization to polynomial and rational splines, were introduced as an easily computable alternative to true splines¹ around the time that industrial design of ships, aircraft and cars moved into the digital environment[7]. True splines, created by thin flexible pieces of wood, held in position at various points, are mathematically described by piecewise planar *elastic curves*, solutions to a nonlinear equation, which are difficult to work with compared to polynomials. It is sometimes said that a *cubic* Bézier curve is quite close to an elastic curve, making them a plausible alternative. This suggestion is based on consideration of the curvature function for a cubic curve that is parameterized by arc-length and not too far from a straight line. However, it is certainly not true that all cubic Bézier curves are close to elastic curve segments: in Figure 1, we have used

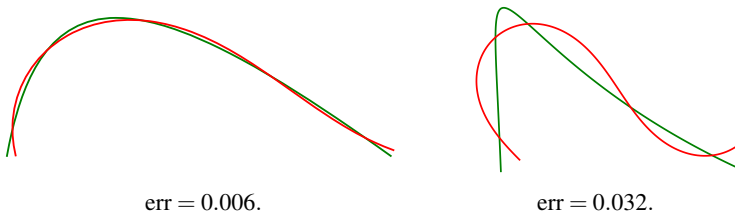


FIGURE 1. Approximations of two cubic Bézier curves (green) by elastic curves (red). The quantity err is the L^2 distance between the Bézier and elastic curve.

the algorithm described in [3] to obtain approximating elastic curve segments (red) for the given Bézier curves (green). Conversely, one can also find elastic curve segments (for example a circle) that are not close to any cubic curve, although the space of all Bézier curves is one dimension higher than the space of elastic curve segments, and most shapes produced by elastic splines can be approximated by cubic splines.

From the CAD point of view, the goal is not necessarily to replicate exactly the behaviour of true splines, and thus polynomial splines are usually a good choice. However, in some cases there are compelling reasons for faithfully representing a true spline in a digital environment: for example if the manufacturing method naturally produces surfaces swept out by elastic curves. An instance of such a method is the recently developed “hot-blade” cutting technology [13], whereby architectural formwork is cut from polystyrene foam using a heated rod, the ends of which are controlled by a

Key words and phrases. Cubic Bézier curves, elastic curves, splines, approximation, computer aided design, physically-based modeling.

¹And other templates such as French curves.

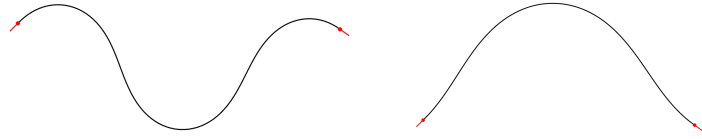


FIGURE 2. Two elastic curves with identical lengths, end points and tangents.

robot. *Rationalization* of a CAD design for this production method means segmenting the surface into suitable pieces and then approximating each segment by a family of planar elastic curves. The primary ingredient for this, an algorithm for approximating an arbitrary curve by an elastic curve segment, is given in [3, 12].

As an alternative to rationalization, we have proposed in [2] a method for using elastic curves themselves in the design process. Unfortunately, true elastic curves can be problematic to work with for a designer. Figure 2 shows two elastic curves of the same length, produced by numerically solving the boundary value problem for elastic curves. Both end points and tangents are (nearly) identical, but the curves are very different despite both having two inflection points.

One could try to make a tool where the designer is allowed to select between such alternatives; but the issue could be side-stepped if a suitable class of cubic Bézier curves can be found, because then the curve is always given uniquely by the control polygon. Besides uniqueness there are further benefits to modeling with cubic Bézier curves instead of actual elastic curves. Importantly, exchanging data between CAD systems is unavoidable when doing real work, and we posit that modeling with an easily transferable format such as splines is a great benefit. Along the same lines, an elastic curve would need to be either converted to a spline or a polyline for any downstream usage – e.g., creating a lofted surface.

In this article, we aim to find conditions on cubic Bézier curves such that curves which fulfill these conditions are very close to elastic curves. These conditions should be easy to make operational as algorithms for turning general cubic Bézier curves into approximate elastic curves. In practical applications, we can then easily obtain precise numeric solutions for the true elastica as a last step.

1.1. Related literature. The energy minimizing (subject to end constraints) property of elastic curves makes them fair from a design point of view, as it is one of the ways to enforce a smooth curvature function. This led to various attempts to emulate this property within a computational setting. One idea is to work with some kind of numeric approximation for elastic curves, e.g. [11], [5], [6], [4]. The drawback of this approach is that it is computationally expensive to solve the boundary value problem associated with an elastic curve; furthermore, as mentioned above, there are issues of non-uniqueness causing instability. This makes an interactive design tool difficult.

A more practical approach is to replace the elastic curves with another class of curves such as energy minimized quadratic [1], cubic [14], or quintic [10] splines, and Pythagorean-hodograph curves [8, 9]. All of these are designed to have low bending energy subject to Hermite interpolation conditions.

Our work does not fit precisely into either of the above viewpoints, because we are not just interested in working with curves of low bending energy, but rather curves that are (visually) close to *actual* elastic curve segments. This is because our practical motivation is to provide a fast, interactive, way to represent physical elastic curves within a CAD system. Therefore, unlike in previous works, our measure of “goodness” for a curve is not its bending energy, but the distance from the closest true elastic curve segment.

1.2. Overview. In Section 2 we briefly introduce results from [3] on approximating an arbitrary curve by an elastic curve and an important quantity that we call the λ -residual, e_λ . This easily computable quantity measures how close the curvature function of a given curve is to the curvature function of an elastic curve. In Section 3 we take a large sample space of cubic Bézier curves and

show that the λ -residual is sufficiently well correlated with the L^2 -distance from the curve to an elastic curve to allow us to use e_λ as a proxy for this distance.

The goal is then to find a method of projecting an arbitrary cubic Bézier curve to a Bézier curve that has e_λ below some threshold. For the sake of concreteness, we aim for $e_\lambda < 0.4$, which corresponds approximately to an L^2 distance less than 0.007, geometrically a deviation of 0.07 percent of the length of the curve. In this work we concentrate on projections that alter only the length of the Bézier curve, keeping the endpoints and end tangent angles fixed. This is grounded in the idea that a tool that allows the user to prescribe exactly the end-points and end-tangents of a curve is most useful for a designer.

In Section 4 we briefly discuss the possibility of gradient driven approaches to projection, i.e., minimizing either the elastic energy or the λ -residual e_λ subject to fixed end-data. This approach is problematic due essentially to the existence of multiple local minima.

In Section 5 we find a large subset Π of cubic Bézier curves, characterized by the end tangent angles, the inner polygon angles and the lengths of the two outer polygon edges, such that e_λ is bounded by 0.4 on Π . We also describe an end-data preserving algorithm for projecting into Π . The results of this section are included partly because the geometric characterization has the possibility of being adapted to other projections if the end-tangent preserving requirement is dropped.

Finally, in Section 6 we present a significantly more effective end-data preserving projection algorithm based on computing the value of e_λ in real time.

2. ELASTIC CURVES AND THE λ -RESIDUAL

An elastic curve is defined to be the minimizer of the *elastic energy* $\int \kappa^2(s) ds$ among curves with given endpoints, end-tangents and length. We refer the reader to [3] for the relevant theory, as well as the details of the approximation algorithm mentioned here. This algorithm uses the well-known analytic description of an elastic curve:

$$\xi_k(s) = (2E(s, k) - s, 2k(1 - \text{cn}(s, k))),$$

where cn is a Jacobi elliptic function,² E is the incomplete elliptic integral of the second kind and $k \in [0, \infty)$. Then any elastic curve segment is, up to a scaling, rotation and translation, given by a piece of some ξ_k . Some examples of these curves are shown in Figure 3.

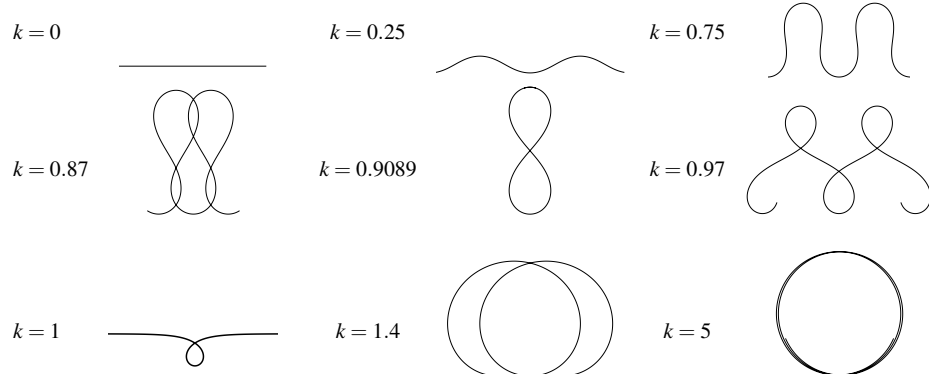


FIGURE 3. Examples of elastic curves.

The approximation algorithm described in [3] takes as input any curve and returns an approximating elastic curve segment. The algorithm consists of two steps:

² Note that this representation uses an extension of the elliptic functions and integrals to $k \in [1, \infty)$ (see [3]), which allows a single formula incorporating the elastic curves both with and without inflections. The limit as $k \rightarrow \infty$ is a circle.

- (1) Obtain a *first guess* elastic curve that has roughly the same shape of the input curve. This exploits the fact that the curvature of an elastic curve is affine in a particular direction, and the first guess is obtained by solving linear least squares problems.
- (2) Apply an optimization to adjust the parameters of the first guess to obtain an optimal solution.

We use this algorithm in this article to obtain an approximating elastic curve segment γ_e for a given Bézier curve γ_B . In the computation of the first guess we find the parameters $\lambda_1, \lambda_2, \alpha \in \mathbb{R}$ that minimize $\int_0^1 (\kappa(t) + \lambda_1 y(t) - \lambda_2 x(t) - \alpha)^2 \frac{ds}{dt} dt$ (this is equivalent to solving a linear system). The associated residual, λ -residual, is given by the formula:

$$e_\lambda = \sqrt{\int_0^1 (\kappa(t) + \lambda_1 y(t) - \lambda_2 x(t) - \alpha)^2 \frac{ds}{dt} dt} \Big/ \sqrt{\int_0^1 \kappa(t)^2 \frac{ds}{dt} dt},$$

where κ is the curvature of the Bézier curve, $s(t)$ is the arclength of the Bézier curve at t .

The λ -residual can be taken as a measure of how much the curvature of a given curve $(x(t), y(t))$ deviates from being the curvature of an elastic curve, and we will use this as one of our tools to analyze Bézier curves. Because the λ -residual can be computed at interactive speeds, it is the most important tool we have for measuring how close a curve is to an elastic curve.

3. THE λ -RESIDUAL AS MEASURE OF CLOSENESS BETWEEN CUBIC BÉZIER CURVES AND ELASTIC CURVES

As our starting point we study a randomized 80,000 sample of cubic Bézier curves to determine useable criteria for identifying those that are close to elastic curves. We take as our initial yardstick the L^2 distance to the approximating elastic curve, which is obtained by the approximation algorithm in [3]. We begin with the criterion that the good Bézier curves are those with an L^2 distance less than 0.01 (i.e., 1 percent of the curve length) from the approximating elastic curve. To ensure the quality of the optimal solution we have applied the elastic curve approximating algorithm using different optimization routines in MATLAB: trust-region, interior point, SQP and Quasi-Newton.

All of our arguments are invariant under scaling, rotation and translation, so we can fix the endpoints of the Bézier curve at $(0, 0)$ and $(1, 0)$ and only vary the two inner control points. Our initial sample space consists of all possible Bézier curves obtained from pairing the red and blue points in Figure 4 and using them as the inner control point pairs. We found approximating elastic curves for all the curves in the sample space, and computed the L^2 error. We then plotted the L^2 distance against the λ -residual, e_λ , defined in Section 2. From Figure 5 we conclude that, for Bézier curves, the λ -residual is well correlated with the L^2 distance to an elastic curve, especially for small values. A maximum L^2 error of 0.01 is achieved by almost all of the curves with $e_\lambda < 0.4$.

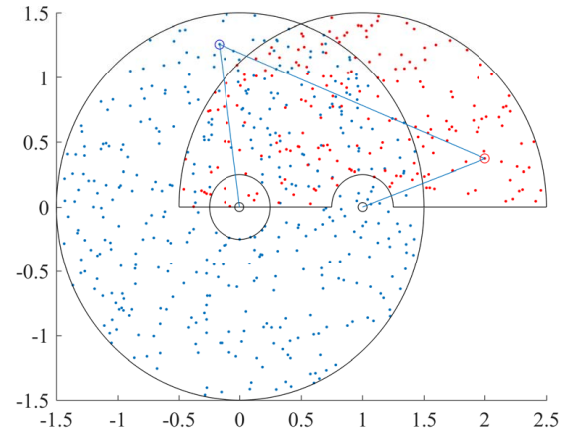
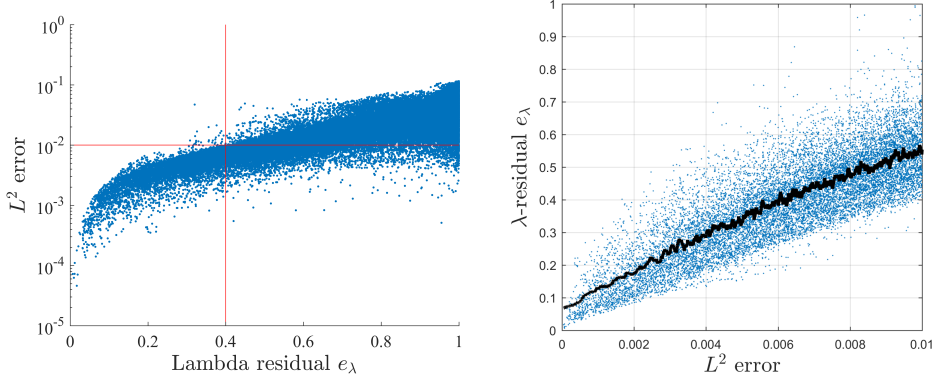


FIGURE 4. Initial sample space of inner control point pairs: one of the 80,000 control polygons is shown for illustration.

FIGURE 5. The λ -residual and L^2 error.

Compared to finding an approximating elastic curve and its L^2 error (via optimization), the λ -residual is easy to compute: we only have to solve a linear system to obtain λ_1, λ_2 and α . Furthermore the λ -residual depends continuously on the control polygon vertices of a spline curve, and is more reliable because the L^2 distance is subject to such factors as the optimization used to find the approximating curve. We therefore use the λ -residual as a more practical measure of closeness to elastic curves. From the trend curve in Figure 5, we apply the following measure of quality:

	Best	Good	Borderline
L^2 error maximum	0.003	0.007	0.01
λ -residual maximum	0.22	0.4	0.5

4. PROJECTION OF CUBIC BÉZIER CURVES: PROBLEMS WITH THE GRADIENT DRIVEN APPROACH

The λ -residual can tell us if a cubic Bézier curve is close to an elastica. This can be used as a diagnostic tool in a design framework. However, if we want to model elastic curves with cubic Bézier curves we need a projection tool for the curves that have a large λ -residual.

In this article we consider only projections that keep the end-points and end-tangents of the curve fixed: that is, given an input Bézier curve, we will modify it only by moving the two inner control points along the line segments between them and their corresponding end-points.

We first consider a gradient driven projection. We have two candidates for the energy to minimize:

- (1) The bending energy $\int \kappa^2 ds$.
- (2) The λ -residual e_λ .

We have implemented and tested a projection tool for both energies. In both cases, we keep the end-points and end-tangent directions fixed and allow the length to vary. With the bending energy we sometimes move towards a curve with a much larger curve length, see Figure 6 left. This means that the projection does not always return a useful Bézier curve. For both energies we have an issue that there is more than one local minimum for the optimization: for example, for given end-points and end-tangent angles, there are often local minimizers to be found both with and without polygon intersections, as well as minimizers corresponding to both inflectional and non-inflectional elastic curves. Figure 6, right, shows an instance of this, where the λ -residual energy was used. From these observations we conclude that the gradient driven approach is unreliable, and/or does not always return a Bézier curve that is close to an elastic curve.

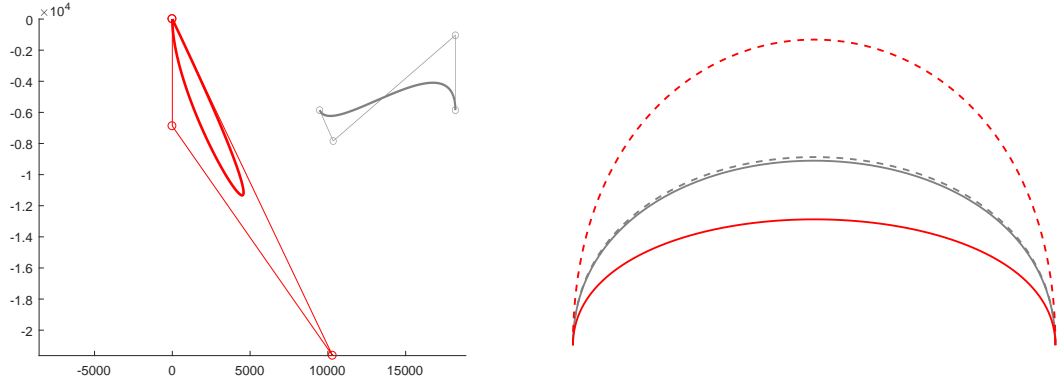


FIGURE 6. Left: input (grey), output (red) after minimizing the bending energy with fixed end tangents directions. Right: two similar inputs (grey) and very different output (red) after minimizing the λ -residual.

5. A PROJECTION BASED ON A GEOMETRIC CHARACTERIZATION OF CURVES WITH LOW λ -RESIDUAL

Due to the problems with the gradient driven approach we now look for a projection tool based on a more geometric characterization of cubic Bézier curves that are close to elastic curves. We will first find criteria in terms of the edge lengths and polygon angles, that guarantee that $e_\lambda \leq 0.4$.

5.1. Finding the projection zone. We first made a large, randomly distributed sample of quadruples of points, p_0, p_1, p_2 and p_3 in the unit disc. Then we scaled and rotated each polygon with $p_0 \mapsto (0,0)$ and $p_3 \mapsto (1,0)$, to get a random collection of Bézier curves in standard position. We reduced the sample space by removing: curves with self-intersecting polygons, and curves that do not satisfy the following angle constraints (see Figure 7):

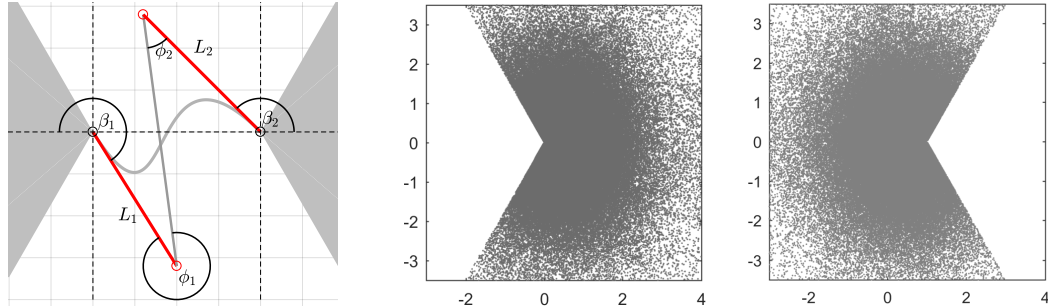


FIGURE 7. Left: Angle constraints: the shaded region is excluded. Extremely asymmetric shapes are excluded by a bound on $|\beta_1 - \beta_2|$. Right: the sample space consists of Bézier curves with endpoints at $(0,0)$ and $(1,0)$ and middle control points all possible pairs with p_1 chosen from the first set shown, and p_2 chosen from the second.

Angle Constraint 1 (absolute angle constraint): $\beta_1, \beta_2 \in (\pi/3, 2\pi - \pi/3)$,

where $\beta_1 \in [0, 2\pi]$ is the angle measured clockwise from the negative x -axis to the first polygon edge, and β_2 is the symmetric analogue for the third edge with respect to the positive x -axis.

Angle Constraint 2 (symmetry constraint): $|\beta_1 - \beta_2| < 0.4\pi$.

The angle constraints are applied because there are relatively few Bézier curves with low λ -residual that do not satisfy them. With the two angle constraints, we are left with 4,330,509 curves containing 434,580 of the “best” curves with $e_\lambda < 0.22$, but 3,187,526 with $e_\lambda > 0.4$, these latter being either unacceptable or borderline unacceptable curves.

Let $\phi_1, \phi_2 \in [0, 2\pi)$ be the angles from the first and third control polygon edges to the second, as shown in Figure 7, left, and L_1 and L_2 denote the lengths of the first and third edges respectively. We look for conditions on these quantities that will remove the bad curves, whilst keeping a large number of good curves. Figure 8 (left) shows a plot of (ϕ_1, ϕ_2) from the sample space, colored by the λ -residual. This shows that (ϕ_1, ϕ_2) alone cannot be used to characterize the good curves. We next include lower and upper bounds on L_1 and L_2 :

Edge-Length Constraint 1: $L_{min} \leq L_1, L_2 \leq L_{max}$,

where

$$\begin{aligned} L_{min} &= \max(0.4(1 + 6\Delta), 0.27), \\ L_{max} &= \max(1.2(1 + 5\Delta), 0.58), \\ \Delta &= \text{sign}(\theta_2) \frac{(\theta_1 - \theta_2)}{\pi}, \end{aligned}$$

θ_i are the two end-tangent angles, measured from the positive x -axis, and we limit the relative lengths of the outer polygon edges:

Edge-Length Constraint 2 (Symmetry for inflectional curves): $\max(L_1/L_2, L_2/L_1) \leq 1.3$, for curve $\phi_2 \leq \pi \leq \phi_1$ or $\phi_1 \leq \pi \leq \phi_2$.

The edge-length constraints were chosen in an ad-hoc manner, based on the observation that we need L_1 and L_2 to be shorter if the legs are angled inward toward the center of the polygon, and longer if angled outwards, and that, for inflectional curves, the better curves have outer edges of similar length.

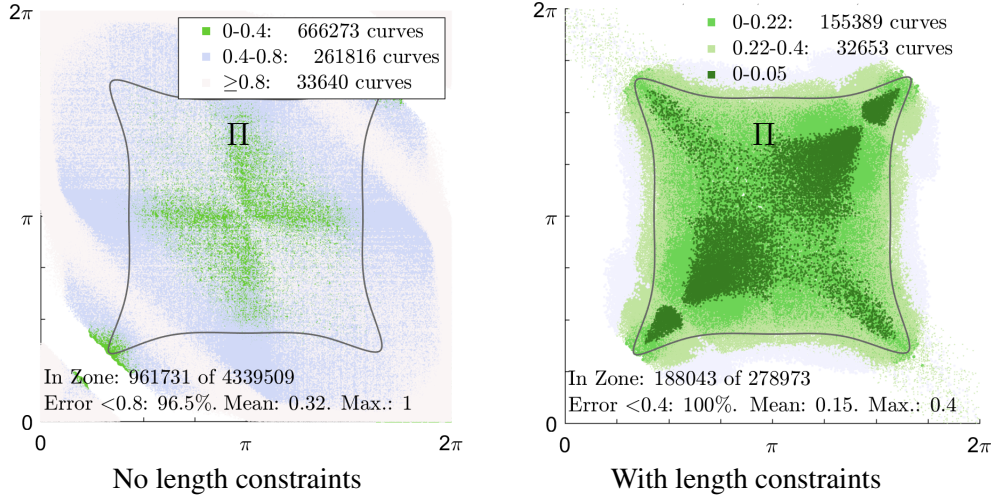


FIGURE 8. Scatter plot of (ϕ_1, ϕ_2) values for the curves in the angle-constrained sample space. Numbers refer to the curves *inside* the projection zone Π bounded by the dark blue curve.

With the edge-length constraints we obtain a bounded region Π (see Figure 8, right) that *only* contains good curves, with a maximum λ -residual of 0.4, whilst retaining 36% of the best curves

$(e_\lambda < 0.22)$. We use this region as a geometrically delineated set of cubic Bézier curves that are close to elastic curves. We define the boundary of Π to be the closed curve given by taking the points $(1.05, 1.05), (1.9, 1.3), (\pi, 1.35), (4.3, 1.3), (5.2, 2\pi - 5.2)$, reflecting them about the line $\phi_1 = \phi_2$, and then about the line $\phi_1 = 2\pi - \phi_2$, and interpolating using a periodic cubic spline interpolation.

5.2. End-tangent angle preserving projection to Π . We now describe, for an input Bézier curve that satisfies Angle Constraints 1 and 2, a projection onto Π that preserves both endpoints and end tangent angles. The only adjustments made to the input curve is to move the two inner control points along the lines between themselves and their corresponding end points (see Figure 9). It follows

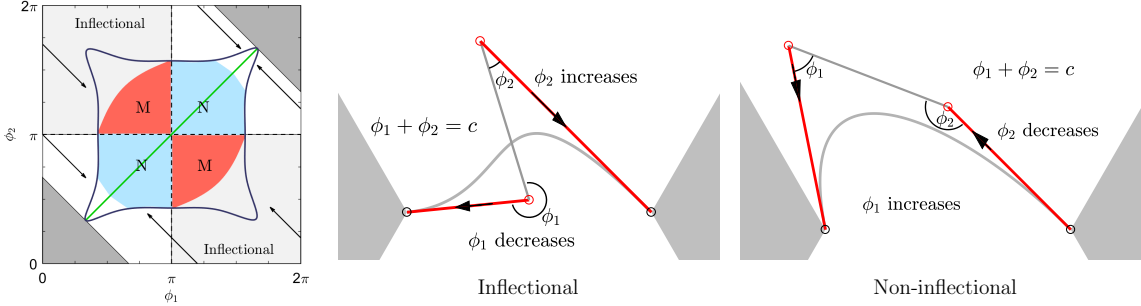


FIGURE 9. End-tangent angle preserving projection. The sum $\phi_1 + \phi_2$ remains constant. For non-inflectional curves, the vertex with the larger angle is moved away from its end-point.

from elementary geometry that the effect of such a motion on the pair (ϕ_1, ϕ_2) of inner polygon angles is to move the pair up and down the line $\phi_1 + \phi_2 = \text{constant}$ on which it lies. We choose to move always in the direction of the arrows in the diagram to the left in Figure 9, i.e., towards the line $\phi_1 = \phi_2$, and it follows that a curve with an inflection can change to a curve without an inflection, but not the other way around.

The projection algorithm is as follows: first remove any self-intersection of the control polygon edges by shortening the outer edge-lengths L_1 and L_2 . Next adjust L_1 and L_2 if necessary so that the edge-length constraints are satisfied (this will not introduce self-intersections). The Bézier curve is then inflectional or non-inflectional depending on the values of (ϕ_1, ϕ_2) , and the following routines are applied for the two cases:

Inflectional Curves ($\phi_2 \leq \pi \leq \phi_1$ or $\phi_1 \leq \pi \leq \phi_2$): We make changes that *decrease* either L_1 or L_2 or both using the deformation

$$(1) \quad L_1(t) = (1-t)L_1 + tL_{\min}, \quad L_2(t) = (1-t)L_2 + tL_{\min},$$

with $t \in [0, 1]$. This moves (ϕ_1, ϕ_2) towards the line $\phi_1 = \phi_2$. The minimal edge length constraint is $L_{\min} = 0.27$ for all relevant inflectional curves, and the locus of (ϕ_1, ϕ_2) that satisfy $L_1 = L_2 = L_{\min}$ is plotted as the red region M in Figure 9, left. This shows that we are guaranteed either to reach the projection zone Π , or that the curve becomes non-inflectional, *before* we arrive at the minimal edge-length constraint.

Non-inflectional Curves ($\phi_1, \phi_2 \leq \pi$ or $\phi_1, \phi_2 \geq \pi$):

- (1) First adjust both L_1 and L_2 if necessary so that Edge-Length Constraint 1 holds.
- (2) Adjust the angles (ϕ_1, ϕ_2) : we describe the case $\phi_1 < \phi_2 \leq \pi$, (the other cases are analogous). Either decreasing L_1 or increasing L_2 (or both) will move (ϕ_1, ϕ_2) towards the line $\phi_1 = \phi_2$ (Figure 9, right image). We decrease L_1 and increase L_2 simultaneously, e.g., with the

formulae

$$(2) \quad L_1(t) = (1-t)L_1 + tL_{\min}, \quad L_2(t) = (1-t)L_2 + tL_{\max},$$

with $t \in [0, 1]$, until the projection zone is reached.

As in the inflectional case, we need to be sure that the projection zone is reached before the edge-length constraints are violated (See Figure 10). Step 2 above can only fail if $\phi_1 < \phi_2$ and if $L_1 = L_{\min}$ and $L_2 = L_{\max}$ (or the analogue for the other positions). To verify that this does not happen we calculate the locus of all such points, and this is plotted as the blue region N in Figure 9. Since N is contained inside Π , the edge-length limits are not exceeded here either.

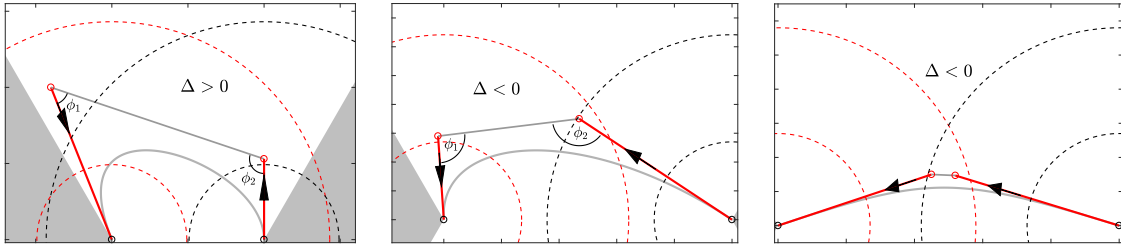


FIGURE 10. Length constraints on the two outer edges when projecting non-inflectional curves.

Finally, note that it is not difficult to verify that no self-intersections are introduced by the above procedures.

5.3. Results of the purely geometry based approach. The above projection algorithm is easily implemented by discretizing the parameter $t \in [0, 1]$, and looping until the projection zone is reached. The projection zone is a compact subset of \mathbb{R}^4 , consisting of a bounded subset of the pairs of middle control points. The λ -residual depends continuously on the control points: we computed the λ -residual for a new set of 10.7 million densely distributed points in the projection zone, and found a maximum of 0.393, confirming the results in Figure 8. Thus we are, with a high level of confidence, guaranteed a result below 0.4 with this method.

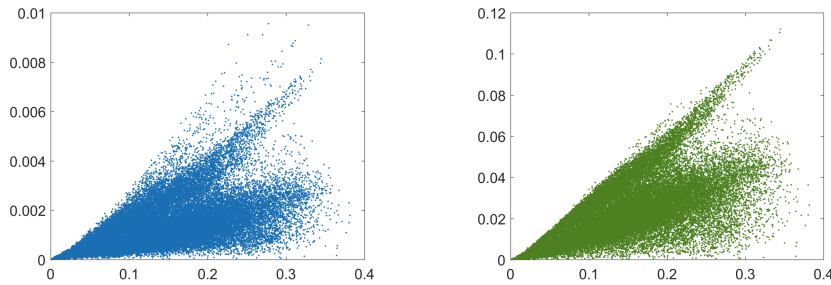


FIGURE 11. Results of optimized L^2 approximations (left) and H^1 approximations (right) for curves in the projection zone. In each case the distance is plotted against e_λ of the input curve.

Finally, to confirm the quality of the curves in the projection zone, we took a random sample of 38,826 curves in this zone and approximated them using the method of [3], both with the L^2 and the

H^1 distances between the Bézier curve γ_B and the elastic curve γ_e :

$$L^2 \text{ distance} : \sqrt{\int_0^1 \frac{\|\gamma_B(t) - \gamma_e(s(t)/L)\|^2}{L^3} \|\gamma'_B(t)\| dt},$$

$$H^1 \text{ distance} : \sqrt{\int_0^1 \frac{\|\gamma_B(t) - \gamma_e(s(t)/L)\|^2}{L^3} \|\gamma'_B(t)\| dt + \int_0^1 (\theta_B(t) - \theta_e(s(t)/L))^2 \frac{\|\gamma'_B(t)\|}{L} dt},$$

where θ_B and θ_e denote respectively the tangent angles of γ_B and γ_e , L is the length of the curve γ_B , and $s(t)$ is the arc-length function for the curve γ_B . The results, plotted against e_λ , are shown in Figure 11. For the L^2 distance, they show that the result is as expected, i.e., the maximum L^2 distance is always less than 0.01, and almost always below 0.007. The H^1 distance shows that an upper bound on e_λ can also be used to obtain an upper bound on the H^1 distance from an elastic curve; this means that we could also use e_λ as a proxy for the H^1 distance.

5.4. Projections that do not preserve end-tangent angles.

Obviously, we can project an arbitrary Bézier curve into Π by first rotating the inner control points about the corresponding endpoints until Angle Constraints 1 and 2 are satisfied and then applying the projection algorithm described above. This would mean dropping the requirement that the output curve has the same end-tangent angles as the input curve. If we do drop the end-tangent preserving condition, then we could expect better results by following the arrows in Figure 5.3 – this differs from the algorithm we have described above in the case of inflectional curves. This alternative appears likely to be more efficient because the scatterplot at Figure 8 (right) suggests that the best inflectional curves are close to the line $\phi_1 + \phi_2 = 2\pi$.

We will not pursue that possibility in this work, because our goal is an end-tangent preserving projection.

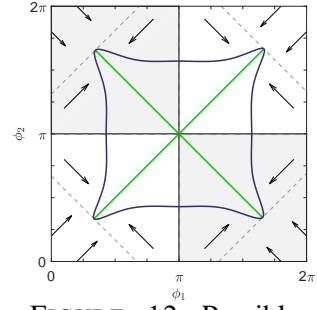


FIGURE 12. Possible alternative projection.

6. A PROJECTION ALGORITHM BASED ON FEEDBACK

Using the projection described above, we obtain a Bézier curve with a maximum value $e_\lambda = 0.4$. However, one finds that 98% of curves score below 0.3. Moreover, there are also curves with very low values of e_λ *outside* the projection zone. Since the λ -residual can be computed easily at interactive speeds, we can obviously improve both the quality of the result (lower value of e_λ) as well as the size of the design space (no need to move all the way into Π in many cases), by computing e_λ on the fly and applying the deformations (1) and (2) until either a threshold level for e_λ is reached or $t = 1$.

Analysis shows that, if we have fixed the end-tangent angles but allow the lengths L_1 and L_2 to vary, then the minimal value of e_λ is close to the boundary of region M for the inflectional curves, and hence it makes sense to use (1) for the inflectional case. For non-inflectional curves the minimal value of e_λ does not occur exactly along the line $\phi_1 - \phi_2 = 0$, so it turns out that we can do better than using (2) for these.

Feedback-based projection algorithm.

- (1) Choose a threshold level $E \in [0, 1)$ for e_λ and a minimum allowed length L_{min} for the outer edges of inflectional curves. We obtained the best results by choosing $L_{min} = 2.7$.

- (2) Scale and rotate so that the control points p_0, p_1, p_2 and p_3 are in standard position, with end-points $p_0 = (0, 0)$ and $p_3 = (1, 0)$. Denote this transformation by T .
- (3) Remove any self-intersection of the polygon edges by reducing the lengths L_1 and L_2 .

Now we classify the curve and adjust L_1 and L_2 :

- 4a. The input curve is classified as **inflectional** if we obtain an inflectional curve after adjusting the outer edges to be within the range $[L_{min}, L_{max}]$, where L_{max} is defined by the same formula as in Edge-Length Constraint 1. In this case, we take the adjusted curve as the input curve, then run the deformation formula (1) until either (a) both L_1 and L_2 are equal to L_{min} , or (b) $e_\lambda \leq E$, or (c) the curve becomes non-inflectional.
- 4b. For **non-inflectional curves**, we choose suitable terminal values \mathcal{L}_1 for L_1 and \mathcal{L}_2 for L_2 (see below). Then adjust L_1 and L_2 according to the formula

$$(3) \quad L_1(t) = (1-t)L_1 + t\mathcal{L}_1, \quad L_2(t) = (1-t)L_2 + t\mathcal{L}_2$$

with $t \in [0, 1]$, until either (a) $L_1 = \mathcal{L}_1$ and $L_2 = \mathcal{L}_2$, or (b) $e_\lambda \leq E$.

5. Finally, apply T^{-1} to the new curve to obtain the projected Bézier curve.

The values \mathcal{L}_i are chosen as local minimizers for e_λ . They depend on the end tangent angles, so should be expressed as $\mathcal{L}_i(\theta_1, \theta_2)$, where θ_i are the angles of the outer edges to the x -axis.

We chose, for $\theta_1 \geq 0$ (i.e. if $y_1 \geq 0$),

$$\begin{aligned} \mathcal{L}_1(\theta_1, \theta_2) &:= \min(0.12, f(\theta_1, \theta_2)), \\ f(\theta_1, \theta_2) &:= 0.00001475 \exp(10.39\theta_1 - 10.48\theta_2) + 0.4574\theta_1 \exp(1.711\theta_1 - 2.535\theta_2) \\ &\quad + 2.772\theta_2 \exp(-0.08504\theta_1 - 0.9109\theta_2) - 0.2957\theta_1\theta_2 \exp(-0.6606\theta_1). \end{aligned}$$

For curves with $y_1 \leq 0$, the corresponding formula is obtained by symmetry, and the formula for \mathcal{L}_2 is also the symmetric analogue. We obtained f by computing local minimizers for a discrete set of (θ_1, θ_2) given by non-inflectional curves that satisfy Angle Constraints 1-2. We then fitted the data using this formula giving a small sum of squares error.

Note: In practice, the algorithm is implemented by discretizing the interval $[0, 1]$. If the threshold E is not reached before the other terminating conditions, then the t -value corresponding to the lowest value of e_λ is chosen as the solution. This ensures that any inaccuracy in the choice of the function f has minimal impact on the result.

Remark 1. *There is no unique or best choice of $\mathcal{L}_i(\theta_1, \theta_2)$, except in the case that the input curve is unambiguously close to either an inflectional or non-inflectional elastic curve. Many input curves are close to both types of elastica, and this leads to two different local minima for e_λ . Therefore, we have made some arbitrary choices in our definition of f above. The impact of these choices is not generally as significant as is the choice of the threshold E .*

6.1. Results of the feed-back based projection. We applied the algorithm, with the threshold set at $E = 0$, to a random sample of 100,000 curves satisfying Angle Constraints 1 and 2. We implemented the algorithm by computing e_λ at $t = 0, 0.1, 0.2, \dots, 1$, taking the solution with lowest e_λ , and then repeating the procedure once. For the projected sample we obtained for e_λ :

$$\text{mean} = 0.048, \quad \text{median} = 0.042, \quad \text{max} = 0.26.$$

The 99th percentile is $e_\lambda = 0.15$, and 99.99% of curves have e_λ less than 0.22. Hence, one could set the target value E to 0.22 and expect the result to always have $e_\lambda \leq E$, or set the target value at 0.15 and expect this result 99% of the time.

Representative examples satisfying Angle Constraints 1 and 2 are shown in Figures 13 and 14. The elastic curve obtained just from the first guest algorithm in [3], (i.e., before any optimization is applied) is also plotted. Note that, if a further optimization is applied to these elastic curves, then they will approximate the projected Bézier curve significantly better.

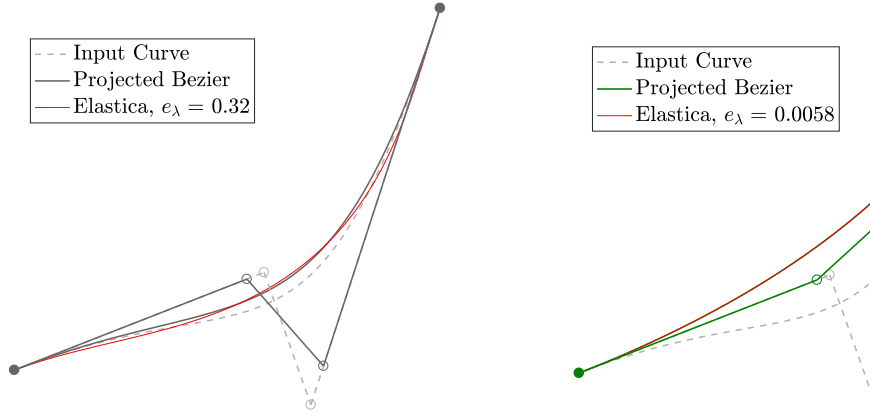


FIGURE 13. Result of the projection algorithm applied with two different choices of threshold level E for e_λ . This example changes from inflectional to non-inflectional. The red curve is the elastica obtained from the first guess.

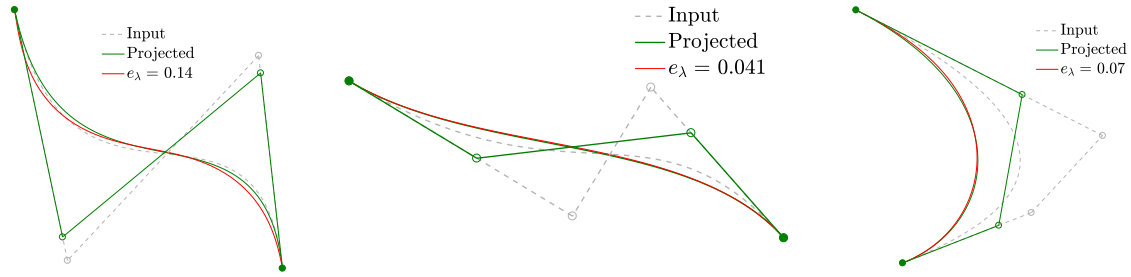


FIGURE 14. Examples of projections. The elastica shown is the first guess.

6.2. Extending the feedback projection to general Bézier curves. A further advantage of the feedback method is that we can apply this projection to any Bézier curve, regardless of the angle constraints, and use the feedback to decide whether or not the projected Bézier curve is close to an elastica. We took a sample of 83,500 arbitrary Bézier curves, each given by 4 randomly chosen control points in the unit disc. Of these, 55% satisfy both Angle Constraints 1 and 2. Applying the projection algorithm (with target $E = 0$) to the curves that do *not* satisfy the angle constraints resulted in a mean for e_λ of 0.4 median of 0.3, and maximum approximately 1. So the projection should not be applied to Bézier curves with no angle constraints at all.

If we replace $\pi/3$ in Angle Constraint 1 by the value $\pi/4$, and replace the value 0.4π by the value 0.6π in Angle Constraint 2, we still obtain good results of

$$\text{mean} = 0.06, \quad \text{median} = 0.043, \quad \text{max} = 0.42,$$

for e_λ in the projected curve. Extending further still to $\pi/6$ and 0.75π respectively produced a mean, median and maximum of 0.1, 0.06 and 0.71 respectively, which is still a useable design space, provided that the feedback is used to reject the input curves that exceed some desired threshold (e.g. those curves above 0.4).

Figure 15 shows some examples of the result of the projection applied to curves that do not satisfy our original angle constraints.

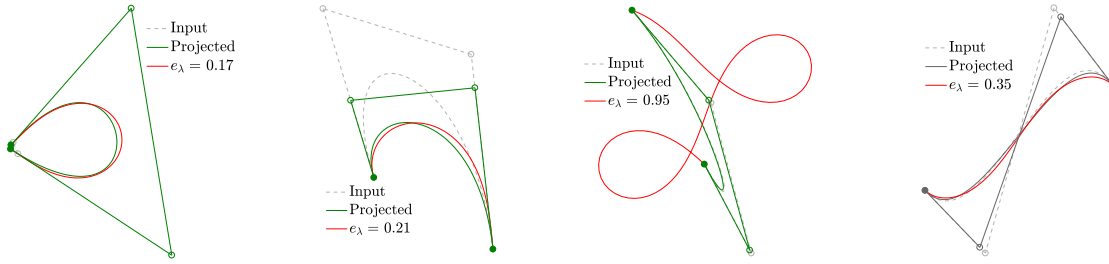


FIGURE 15. Examples that do not satisfy Angle Constraint 1 (left two), and Angle Constraint 2 (right two).

7. CONCLUSION AND FUTURE WORK

We have shown statistically that the λ -residual gives a convenient, easily computable, way of measuring closeness to an elastic curve. Based on this we have defined a reliable feedback-based projection algorithm that takes an arbitrary cubic Bézier curve as input and adjusts the length to produce a new cubic Bézier curve with the same endpoints and end-tangent angles. If the end-tangent angles of the input curve satisfy our angle constraints, then the output curve is guaranteed to be close to an elastic curve. For arbitrary Bézier curves, the end-tangent angles can be rotated first if necessary. An implementation in MATLAB of the feedback based projection algorithm can be downloaded (at time of writing) from <http://geometry.compute.dtu.dk/software/> and tested.

A version of the projection algorithm described here has been incorporated into a hot-blade cutting design tool implemented in Rhino/Grasshopper, extending the work described in [2]. This allows architects to design fabrication-ready surfaces for hot-blade produced concrete casting. The benefit of using elastica-like Bézier curves is that the designed surface is visually the same as the surface that will actually be produced.

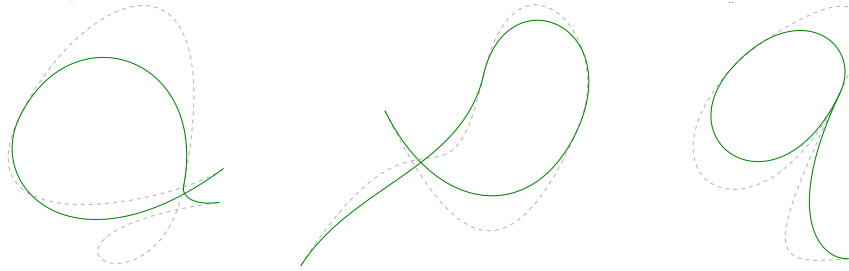


FIGURE 16. Examples of C^1 cubic splines where each of 3 segments is close to an elastic curve.

The projection algorithm can be used to construct C^1 splines that are close to elastic splines, see Figure 16. However, for splines, a different method that allows end-points and end-tangents to be adjusted in addition to length is likely to be more suitable, and this will be studied in future work.

ACKNOWLEDGEMENTS

Research partially supported by Innovation Fund Denmark, project number 91-2014-3.

REFERENCES

[1] Y.J. Ahn, C. Hoffmann, and P. Rosen, *Geometric constraints on quadratic Bézier curves using minimal length and energy*, J. Comput. Appl. Math. **255** (2014), 887–897.

- [2] D. Brander, J.A. Bærentzen, K. Clausen, A. Fisker, J. Gravesen, M. Lund, T. Nørbjerg, K. Steenstrup, and A. Søndergaard, *Designing for hot-blade cutting: geometric approaches for high-speed manufacturing of doubly-curved architectural surfaces*, Advances in Architectural Geometry 2016, Hochschulverlag AG an der ETH Zurich, 2016, pp. 306–327.
- [3] D. Brander, J. Gravesen, and T. Nørbjerg, *Approximation by planar elastic curves*, Adv. Comput. Math. (2016) **43** (2016), 25–43.
- [4] A.M. Bruckstein, R.J. Holt, and A.N. Netravali, *Discrete elastica*, Discrete Geometry for Computer Imagery: 6th International Workshop, DGCI’96 (Lyon, 1996) (Berlin, Heidelberg) (S. Miguet, A. Montanvert, and S. Ubéda, eds.), Springer, 1996, pp. 59–72.
- [5] Guido Brunnett and Johannes Kiefer, *Interpolation with minimal-energy splines*, Comput. Aided Design **26** (1994), no. 2, 137–144.
- [6] John A. Edwards, *Exact equations of the nonlinear spline*, ACM Trans. Math. Softw. **18** (1992), no. 2, 174–192.
- [7] G. Farin, *A history of curves and surfaces in CAGD*, Handbook of computer aided geometric design, North-Holland, Amsterdam, 2002, pp. 1–21.
- [8] R. Farouki, *The elastic bending energy of Pythagorean-hodograph curves*, Comput. Aided Geom. Design **13** (1996), no. 3, 227–241.
- [9] ———, *Construction of G^1 planar Hermite interpolants with prescribed arc lengths*, Comput. Aided Geom. Design **46** (2016), 64–75.
- [10] L. Lu, *Planar quintic G^2 Hermite interpolation with minimum strain energy*, J. Comput. Appl. Math. **274** (2015), 109–117.
- [11] E. Mehlum, *Nonlinear splines*, Comput. Aided Geom. Design (Proc. Conf., Univ. Utah, Salt Lake City, Utah, 1974) (R.E. Barnhill and R.F. Riesenfield, eds.), Academic Press, 1974, pp. 173–207.
- [12] T.B. Nørbjerg, *Rationalization in architecture with surfaces foliated by elastic curves*, Ph.D. thesis, Technical University of Denmark (DTU), 2016.
- [13] A. Søndergaard, J. Feringa, T. Nørbjerg, K. Steenstrup, D. Brander, J. Gravesen, S. Markvorsen, J.A. Bærentzen, K. Petkov, J. Hattel, K. Clausen, K. Jensen, L. Knudsen, and J. Kortbek, *Robotic hot-blade cutting*, Robotic Fabrication in Architecture, Art and Design 2016 (D. Reinhardt, R. Saunders, and J. Burry, eds.), Springer International Publishing, 2016, pp. 150–164.
- [14] J.-H. Yong and F. Cheng, *Geometric Hermite curves with minimum strain energy*, Comput. Aided Geom. Design **21** (2004), 281–301.

DEPARTMENT OF APPLIED MATHEMATICS AND COMPUTER SCIENCE, MATEMATIKTORVET, BUILDING 303 B,
TECHNICAL UNIVERSITY OF DENMARK, DK-2800 KGS. LYNGBY, DENMARK

E-mail address: dbra@dtu.dk

E-mail address: janba@dtu.dk

E-mail address: ansofi@dtu.dk

E-mail address: jgra@dtu.dk